Research article

Network pharmacology, molecular docking and experimental approaches of the anti-proliferative effects of *Rhamnus prinoides* ethyl-acetate extract in cervical cancer cells

Sally Wambui Kamau [a,b,*], Mathew Piero Ngugi [b], Peter Githaiga Mwitari [a], Sospeter Ngoci Njeru [a,**]

[a] *Center for Traditional Medicine and Drug Research, Kenya Medical Research Institute, Kenya*
[b] *Department of Biochemistry, Microbiology and Biotechnology, Kenyatta University, Kenya*

A B S T R A C T

Background: Cervical cancer, one of the lethal cancers among women, is a challenging disease to treat. The current therapies often come with severe side effects and the risk of resistance development. Traditional herbal medicine, with its potential to offer effective and less toxic options, is a promising avenue. This study was undertaken to investigate the potential of *Rhamnus prinoides* (*R. prinoides*) root bark extracts in selectively inhibiting the proliferation of cervical cancer cells, using the HeLa cell line as an *in vitro* model.

Methods: R. prinoides plant extracts were first screened at a fixed concentration of 200 μg/ml to determine the active extract. The selective anti-proliferative activity of the active extract was evaluated in a concentration dilution assay using the (3-(4,5-dimethylthiazol- 2-yl)-2,5-diphenyl-tetrazolium bromide) MTT assay on cancerous (HeLa) cells and non-cancerous (Vero) cells to determine the half-maximal inhibitory (IC_{50}) and half-cytotoxic concentrations (CC_{50}), respectively. Functional assays on cell morphology (by microscopy), cell migration (wound healing assay) and cell cycle (by flow cytometry) were also conducted. The active extract was analyzed using Gas Chromatography/Mass Spectrometry (GC/MS) to determine any compounds it contained. Following identification of possible gene targets by network pharmacology, the genes were validated by molecular docking and Real-Time Quantitative Polymerase Chain Reaction (RT-qPCR).

Results: The ethyl acetate extract of *R. prinoides* (EARP), the most active extract, selectively inhibited the growth of cervical cancer cells, their migration and induced cell cycle arrest at the S phase. *In silico* analysis revealed that squalene, 3,3a,6,6-tetramethyl-4,5,5a,7,8,9-hexahydro-1H-cyclopenta[i]indene and Olean-12-en-3.beta.-ol, acetate showed acceptable drug-like characteristics and may be partly attributed to the bioactivity demonstrated and the deregulation of the mRNA expression of AKT1, NF-κB, p53, Bax, Bcl-2, and Er-b-B2.

Conclusion: This study, for the first time, demonstrates the anti-proliferation effects of EARP and forms a firm foundation for further drug development studies.

 * Corresponding author.
 ** Corresponding author.
    E-mail addresses: salliekamau@gmail.com (S.W. Kamau), snjeru@kemri.go.ke (S.N. Njeru).

1. Introduction

Worldwide, the most frequent cause of fatalities is cancer, which has even been hailed recently as a "major public health challenge". After lung, colorectal, and breast cancers, respectively, cervical cancer comes fourth in terms of prevalence. The bulk of new instances and fatalities from cervical cancer occurs in low-to-middle-income nations, which bear a disproportionate amount of the burden when compared to nations with higher income; actually, 84 % of all cervical cancer cases worldwide are found in Sub-Saharan Africa [1]. Cervical cancer accounts for 12.4 % of all malignancies in Kenya, coming second in terms of prevalence, nevertheless, being the primary cause of cancer-related loss of life in the nation, accounting for 11.9 % of all cancer-related deaths, with breast cancer, which is first in terms of prevalence, accounting for 11.5 % of all cancer-related deaths. Factors such as inadequate health facilities, personnel and late diagnosis are responsible for the increased prevalence and high mortality rates [1–4]. Cytoreductive surgery, radiation therapy, and chemotherapy are the most widely used treatment options for cervical cancer in Kenya. The high cost of treatment along with high instances of recurrence, chemo-resistance and severe side effects, are some of the problems associated with the chemotherapy [5,6]. Thus, searching for less harmful and more effective alternatives is both necessary and essential.

Traditionally, use of therapeutic plants, dates back a long way in treating and mitigating illnesses, and they hold a vast potential as reservoirs of potent anti-cancer agents [7,8]. *Rhamnus prinoides* L'Herit (*R. prinoides*), which belongs to the genus Rhamnaceae, is a plant exotic to Kenya and native to many parts of Eastern and Central Africa. The tree is small, attaining an average height of just 4 m. It is known locally as "Mukarakinga" among the Kikuyu community and "Olkonyil" among the Maasai community in Kenya. Traditionally, a variety of plant parts of *R. prinoides* are used, these include, the leaves, stembark, and root bark, to address chest issues, tonsils, pneumonia, as an appetizer, to manage malaria, sexually transmitted diseases, and to cleanse blood, depending on the region [9–12]. *R. prinoides* extracts were shown to have anti-microbial qualities [13], anti-oxidant properties [14,15], anti-malarial effects [16], and anti-inflammatory action [15]. To the best of our knowledge, *R. prinoides* anti-proliferation and anti-cancer activities have not been assessed experimentally.

We sought to explore the potential of anti-proliferation of crude-, hexane-, water- and ethyl acetate extracts of *R. prinoides* against human cervical cancer cells (HeLa cells) and non-cancerous *Cercopithecus aethiops* epithelial line from African green monkey kidney cells (Vero cells). The results demonstrated that the ethyl acetate extract fraction (EARP) exhibited the most effective selective action towards cervical cancer. We identified the compounds in the extracts that can be partly attributed to the recorded bioactivity using GC/ MS analysis. We then conducted *in silico* studies which suggested that certain compounds had promising putative binding affinities with various genes essential for the development and progression of cervical cancer. We further validated these findings through *in silico* docking studies, cellular functional assays (ability to limit cell migration and induce cell cycle arrest at the S phase) and by gene expression analysis using RT-qPCR. Notably, we found that EARP down-regulated the mRNA expression of AKT1, Bcl-2 NF-κB and Er-b-B2 genes while up-regulating the m-RNA expression of tumor suppressor protein 53 and Bax.

Therefore, we showed the potential of *R. prinoides* ethyl acetate extract as an anti-cancer agent and laid a solid foundation for further studies to isolate the compounds responsible for activity and validate their activity in higher organisms.

2. Materials and methods

2.1. Plant collection and extraction

2.1.1. Plant collection

The root barks of *R. prinoides* were fetched from the region of Mount Kenya at the coordinates 0° 07′ 15.60″ N, 37° 20′ 7.20″ E. A taxonomist assisted in the plant's identification, collection and a voucher specimen was archived in the National Museums of Kenya's East Africa Herbarium (Mwitari/Gathiuru/RM/001/2022). The root barks were sent to the Kenya Medical Research Institute's Center for Traditional Medicine and Drug Research for processing and extraction.

2.1.2. Plant preparation

After the root barks were cleaned to get rid of dust and other particles, they were chopped into smaller bits and allowed to air dry at room temperature then crushed into a powder with a laboratory mill [17].

2.1.3. Solvent extraction

The cold solvent extraction method followed by solvent partitioning was used as described previously with minor adjustments [18, 19]. 800g of the ground root bark of *R. prinoides* was weighed using a laboratory electric balance and macerated in dichloromethane: methanol mixture in a 1:1 ratio until submerged for 72 h with occasional shaking to get a crude extract. The solvent mixture was then decanted into a conical flask with a Whatman No.1 filter (Schleicher and Schuell Microscience Gmbh, Germany) and a vacuum rotary evaporator (Buchi, Switzerland) used to condense the extract at 55 °C. A portion of the crude extract was allowed to air dry. The remaining crude extract was re-soaked in 400 ml hexane to extract the non-polar compounds and concentrated in a rotary evaporator at 59 °C and allowed to dry at room temperature.

Furthermore, the remaining extract was soaked in a combination of water and ethyl acetate in a 1:1 ratio in a separating funnel to extract the mid-polar and the polar compounds. The mixture was left to separate overnight forming two distinct layers. The two layers were then separated using density. The ethyl acetate partition was concentrated in a vacuum rotary evaporator at 67 °C while the water partition was lyophilized in a freeze drier (Modulyo Edwards high vacuum, Crawley England, Britain, Serial No. 2261). The extracts were left to air dry and kept at −20 °C until use. The percentage yield of the crude-, hexane-, water- and ethyl acetate extracts was

calculated as;

% yield = [(weight of dried extract) / (weight of dried plant sample)] x 100

With the use of an electric balance, 100 mg each plant extract fraction was measured and dissolved in 1 ml of laboratory-grade 100 % Dimethyl Sulphoxide (DMSO, FINAR, India) and kept at −20 °C until use as the stock solution.

2.2. Cell culture and anti-proliferation assay

2.2.1. Cell culture

The American Type Culture Collection (ATCC) supplied the non-cancerous Vero cells (ATCC Cat# CCL-81, RRID: CVCL_0059) and cervical cancer HeLa-229 cells (ATCC Cat# CCL-2.1, RRID: CVCL_1276) that were used for the experiments. The MycoStrip™ Mycoplasma Detection Kit (Invitrogen, USA) was used to ascertain the purity of the cell lines. 10 % Fetal Bovine Serum (FBS, Sigma Aldrich, USA) was added to the Minimum Essential Medium (MEM, GIBCO, USA) along with 7.5 % Sodium Hydrogen Carbonate (LOBA Chemie, India), 1 % L-Glutamine (Sigma Aldrich, USA), 1 % Penicillin/Streptomycin (Sigma Aldrich, USA) and 1 % HEPES buffer (Gold Biotechnology, USA). They were maintained at 37 °C with 5 % CO_2 inside an incubator with humidity (Thermo Fisher Scientific, USA).

2.2.2. Viability and proliferation assay

Proliferation and viability of HeLa and Vero cells was determined using the MTT assay as described previously [20]. In brief, HeLa and Vero cells were seeded at a density of 10,000 cells/well in 96 well plates (Thermo Fisher Scientific, USA) and left overnight to grow at 37 °C with 5 % CO_2 in an incubator with humidity. After 24 h, the used media was dispensed with and replenished with 100 μl of fresh media. The plant extract concentrations were made by diluting the initial stock, reconstituted with DMSO, using growth media with the final DMSO concentration being 0.4 %. The first screening was conducted on water-, crude-, hexane- and ethyl acetate extracts and also doxorubicin hydrochloride as a positive control at a fixed concentration of 200 μg/ml for 48 h in HeLa cells. 0.4 % DMSO was used as a negative control. The most active extract was selected and the cells were treated to a range of concentrations of the active extract (starting from 240 to 0 μg/ml in HeLa and 800-0 μg/ml in Vero cells) for 48 h. The positive control utilized was doxorubicin hydrochloride at concentrations starting from 10 to 0.5 μg/ml for HeLa cells and 100–1.5625 μg/ml for Vero cells. The media with the extract was then discarded and the cells washed lightly using phosphate-buffered saline (PBS, Sigma Aldrich, USA). Thereafter, fresh media containing MTT dye (Solar Bio, China) at a concentration of 5 mg/ml in PBS was put in and the plates incubated for 4 h at 5 % CO_2 and 37 °C. After 4 h the formation of formazan crystals was confirmed through the change in color from yellow to purple. The media was dispensed with and 100 μl of DMSO put into the wells and the absorbance read at 570 nm and 720 nm was used reference wavelength to capture non-specific absorbance in a microtiter reader (Thermo Fisher Scientific, USA). The experiment was run in triplicate at least three times. The anti-proliferation effect of the extract was expressed as a percentage of the ratio of the treated cells to those treated with the negative control and the IC_{50} (Inhibitory concentration that kills 50 % of cells), IC_{25} and $IC_{12.5}$ values were estimated with the Graph pad Prism 8.0 software (La Jola, California, USA).

% Viability = [Absorbance of Sample/Absorbance of Control] *100

2.3. Cell phenotypic analysis

To delve into how the EARP extract affects the morphological phenotype of HeLa cells, for 48 h the cells were treated with EARP at IC_{50}, IC_{25} and $IC_{12.5}$ concentrations and the positive control, doxorubicin hydrochloride, at its IC_{50} concentration. The resulting phenotypic changes were recorded using an EVOS™ XL Core Imaging system (Thermo Fisher Scientific, USA).

2.4. Wound healing assay

The effect of EARP on the limitation of HeLa cells migration was estimated according to the previously described method [21]. HeLa cells were seeded in 24-well plates and left to attach overnight in a humidified incubator at 37 °C with 5 % CO_2. An artificial wound was made by use of a sterile p200 tip once a confluent monolayer had been formed. After scraping the cells and washing away loose cells with PBS, new media containing the EARP extract at its IC_{50}, IC_{25} and $IC_{12.5}$ concentrations was added to the wells. Using an ultra-fine tip marker pen (Sharpie, USA), a reference line was made perpendicular to the artificial wound. The scratch areas were captured at 0 h, 24 h and 48 h using an EVOS™ XL Core Imaging system (Thermo Fisher Scientific, USA) and analyzed using Image J software (imagej.nih.gov). The percentage wound closure was calculated using the formula:

%Wound Closure = [(A (0) - A (t))/A (0)] × 100

Whereby, A (0) is the area at time zero (0) and A (t) is the area after incubation time (t).

2.5. Cell cycle analysis

In order to examine how EARP affects the cell cycle, HeLa cells at 100,000 cells/ml were propagated in T-25 culture flasks using MEM culture media and incubated overnight at 37 °C with 5 % CO_2. The cells were then exposed to EARP at IC_{50}, IC_{25} and negative control and incubated for 48 h at 37 °C with CO_2 at 5 %. Thereafter, trypsin was used to harvest the cells after they had been incubated and rinsed twice with ice-cold PBS. Then cells were suspended in 70 % ethanol for 24 h. After discarding the ethanol, the cells were centrifuged for 2 min at 2000 rcf and re-suspended in PBS with 0.25 % Triton X-100 for 15 min on ice. After centrifugation of the cells for 2 min at 2000 rcf, the supernatant was discarded. The cells were kept at 24 °C for 30 min in a dark place after being re-suspended in PBS with 10 μg/ml of RNase A and 25 μg/ml of propidium iodide. A flow cytometer (BD Canto II, BD Sciences) was used for recording and analysis done using FlowJo software (version 10.7.0), to determine the distribution of the cell cycle at G1, S and G2/M phases [21].

2.6. Phytochemical screening of EARP

The color based phytochemical screening tests of EARP were done according to standard methods [14,22].

2.6.1. Test for alkaloids
Half a gram of plant extract was weighed and stirred in 2 ml of 1 % aqueous hydrochloric acid and heated in a boiling water bath for 10 min. The mixture was filtered while hot and treated with Dragendorff`s reagent. Turbidity or precipitation was used to indicate the presence of alkaloids.

2.6.2. Test for terpenoids
Half a gram of the extract was defatted with hexane. The residue was then extracted in dichloromethane and the solution dehydrated with magnesium sulfate anhydride. The mixture was treated with 0.5 ml acetic anhydride followed by addition of 2 drops of concentrated sulphuric acid. A gradual appearance of green blue color was used to indicate presence of sterols while color change from pink to purple indicated the presence of triterpenes.

2.6.3. Test for saponins
Half a gram of the plant extract was dissolved in 5 ml of distilled water and shaken for at least 5 min. Persistent frothing for at least half an hour indicated the presence of saponins. The quantity of froth was used to estimate quantity.

2.6.4. Test for flavonoids
Two hundred milligrams of the extract was dissolved in 4 ml of 50 % methanol. The solution was warmed and then metal magnesium added. Five drops of concentrated sulphuric acid was added. Development of a red color indicated the presence of flavonoids while orange color showed presence of flavones.

2.6.5. Test for tannins
The ferric chloride test was used. Half a gram of the extract was dissolved in 2 ml of distilled water and filtered. Two drops of ferric chloride was added to the filtrate. Development of a blue-black precipitate indicated the presence of tannins.

2.6.6. Test for phenols (ferric chloride test)
2 ml of distilled water was added to 1 mg of plant extract followed by a few drops of 10 % aqueous ferric chloride solution. Formation of blue or green color indicated the presence of phenols.

2.6.7. Test for glycosides
2 mg of plant extract was dissolved in 1 ml distilled water and then aqueous sodium hydroxide was added. Formation of a yellow color indicated the presence of glycosides.

2.7. Gas Chromatography/Mass Spectrometry (GC/MS) of EARP

The compounds contained in EARP were identified through GC/MS QP-2010SE instrument (Shimadzu, Kyoto, Japan) with a BPX5 capillary column with dimensions 30m *0.25 mm * 0.25 μm film in width with a low polarity. In order to reach the isothermal temperature of 280 °C and maintain it for 15 min and 30 s, the oven was configured to start at 50 °C and stay that way for 1 min before progressively raising the temperature by 10 °C per minute. The injector's temperature was retained at 200 °C and its flow rate at 1.08 mL per minute. Helium was used as the carrier gas. As AS30000 auto-sampler connected to a GC in split mode with a split ratio of 10:1 automatically injected 1 μl of the diluted sample in solvent after a 4 min delay. The source of the ions and interface were adjusted to 250 °C and 200 °C, respectively. In full scan mode, the EI mass spectra above the range of m/z 35–550 and at 70 eV were then fetched. The chemical components in the extract were identified using the mass spectrum database of the National Institute of Standards and Technology (NIST) [23].

2.8. *In silico studies*

2.8.1. *Drug screening*

PubChem (https://pubchem.ncbi.nlm.nih.gov/) was utilized to generate canonical SMILES of chemical compounds identified through GC/MS. Their ADMET (Absorption, Distribution, Metabolism, Excretion and Toxicity) attributes were gotten using the Swiss ADME online database (http://www.swissadme.ch/index.php) and the pkCSM tool (http://structure.bioc.cam.ac.uk/pkcsm). The parameters that were described in these databases were used to project the drug-likeness of the compounds on the basis of the following criteria: Lipinski's rule of five (molecular weight in Daltons <500, log P o/W, hydrogen bond acceptors ≤10 and hydrogen bond donors ≤5), oral bioavailability; interaction with cytochromes; crossing the blood-brain barrier (BBB) as well as the topological surface area (TPSA) [24,25].

2.8.2. *Identification of therapeutic targets*

Genes associated with cervical cancer were assembled using Gene Cards (https://www.genecards.org/), DISGeNET (https://www.disgenet.org/), OMIM (https://www.omim.org/) and NCBI (https://www.ncbi.nlm.nih.gov/gene) databases with the phrase "cervical cancer" being the key word. All the results were merged and the duplicates were removed. Targets from EARP were gotten from Swiss Target Prediction (http://www.swisstargetprediction.ch/), Similarity Ensemble Approach (SEA) (https://sea.bkslab.org/) and Super-PRED (https://prediction.charite.de/subpages/target_prediction.php) databases. The gene ids were acquired from the Universal Protein Resource (Uniprot), (https://www.uniprot.org/). The outputs from the databases was put together and duplicates were deleted. Common genes between the targets and the cancer genes were gotten from an online Venn diagram generator (https://bioinformatics.psb.ugent.be/webtools/Venn/) [26].

2.8.3. *Generation of the protein-protein interaction (PPI) network*

The similar genes were loaded into the STRING 12.0 database (https://string-db.org/), where the minimum threshold was set at 0.4. Cytoscape software (version 3.10.2) was utilized to analyze the topology based on the degree of centrality with the Cytohubba plug-in being used to generate the top 30 genes based on five centralities, MCC (Maximal Clique Centrality), ECC (Eccentricity), BN (Betweenness), DG (Degree) and CN (Closeness).

2.8.4. *Gene ontology (GO) and Kyoto Encyclopedia of genes and Genomes (KEGG) enrichment analysis*

The online enrichment tool Shiny GO version 0.80 (http://bioinformatics.sdstate.edu/go/) was utilized to conduct these studies [27]. The parameters set were; species was "Human", false discovery rate (FDR) cut-off was 0.05 and the number of pathways displayed were up to 20 [22].

2.9. *Molecular docking*

3D Structured Data File (SDF) format of the compounds selected after ADMET parameters were analyzed were gotten from Pub-Chem database. The RCSB protein database (https://www.rcsb.org/) was used to get the structures of the proteins of the top 30 genes. The filters applied were; the species was Human, the experimental method was X-ray Diffraction, the resolution was between 0.5 and 3.5 Å and the structure determination methodology was experimental. Using Discovery Studio 2021, the targeted proteins were curated whereby the Gasteiger charges were added, water molecules were removed, all co-crystallized ligands removed and polar hydrogen were added. The 3D SDF compounds (ligands) were edited and transformed into the "pdbqt" format with the aid of the inbuilt Open Babel software in Pyrx program ((https://sourceforge.net/projects/pyrx/). The embedded Autodock Vina software in Pyrx program was then used to dock the prepared ligands to the prepared proteins. The size of the protein was used to centralize the three-dimensional grid box. Discovery studio 2021 (https://discover.3ds.com/discovery-studio-visualizer-download) was used to generate the 3D protein-ligand complexes with the lowest binding energies and their 2D interaction diagrams [28].

2.10. *Survival analysis*

Some of the genes with the lowest binding affinities were assessed with the aid of the GEPIA database (http://gepia.cancer-pku.cn)

Table 1
Forward primers and reverse primers of genes used.

GENES	FORWARD PRIMERS	REVERSE PRIMERS
P53	CTTCGAGATGTTCCGAGAGC	GACCATGAAGGCAGGATGAG
EGFR	TCTGGAAGTACGCAGACGCC	TGGGAGACTAAAGTCAGACAGTG
Er-b-B2	TGGGAGCCTGGCATTTCTGC	TGTGCAGAATTCGTCCCCGGATTA
BAX	CAGAGGATGATTGCCGCCG	AAAAGGGCGACAACCCGGCC
BCL2	GGCCTCAGGGAACAGAATGAT	TCCTGTTGCTTTCGTTTCTTTC
AKT1	CCATCTGTCACCAGGGGCTT	ATAGCCACGTCGCTCATGGT
NF-κB	CGCTTAGGAGGGAGAGCCCA	TGCCATTCTGAAGCTGGTGGT
GAPDH	AGACAGCCGCATCTCTTG	TGACTGTGCCGTTGAACTTG
β-ACTIN	GCCAACTTGTCCTTACCCAGA	AGGAACAGAGACCTGACCCC

to ascertain the correlation between their expression and overall patient survival and overall disease free survival [29].

2.11. RNA isolation and quantification using RT-qPCR

To validate the docked proteins as well as assess the effect of the EARP extract on key oncogenic genes, RT-qPCR was used. HeLa cells were seeded in T-75 culture flasks and upon attaining a confluence of >70 %, they were treated with the EARP extract at IC_{50} concentration for 48 h. After treatment, the flasks were rinsed with PBS thrice and RNA was obtained using the Pure Link™ RNA Mini Kit (Thermo Fisher Scientific, USA) extraction kit. A NanoDrop, ND-2000 spectrophotometer (Thermo Scientific, USA), was employed in the quantification of the extracted RNA. The RNA was preserved at −80 °C until use. 1 μg of RNA was converted to cDNA using the Firescript® RT cDNA synthesis kit (Solis Biodyne, Estonia). The cDNA was stored at −20 °C until use. The genes used were purchased from Macrogen (Macrogen, South Korea), (Table 1). The HOT Firepol® Evagreen® qPCR Mix plus (ROX) (Solis Biodyne, Estonia) was utilized for quantitative RT-qPCR analysis using the Quant Studio™ 5 RT-qPCR system (Applied Biosystems, USA). A blank containing the master mix and the primers without the cDNA was used. Analysis of the melt curve verified that there was no non-specific binding. The targeted genes' mRNA levels were quantified using the $2^{-\Delta\Delta Ct}$ method. GAPDH and β-actin controls were the internal references [17].

2.12. Statistical analysis

The data was expressed as mean ± standard deviation (mean ± SD). One-way ANOVA using Dunnett's multiple comparison test was employed to show the differences in different groups. A p-value of less than 0.05 was used to show statistical significance for every statistical test. Graph Pad Prism 8.0.2 (La Jola, California, USA) software was used for analysis.

3. Results

3.1. Percentage yield of R. prinoides extracts

We used the percentage yield after extraction to estimate the abundance of the extracts in the root bark of the plant according to the formula described above. The percentage yields were 1.39 % from the crude extract, 0.5 % from the hexane extract and 0.39 % from the water and ethyl acetate extract (Table 2). The greatest yield was obtained from the crude extract.

3.2. Selective anti-proliferation activity of EARP

We first screened the crude-, hexane-, ethyl acetate- and water extracts as well as the positive control at a fixed concentration of 200 μg/ml and the extract that inhibited cell proliferation by ≥ 50 %, was selected for further evaluation (Fig. 1). *R. prinoides* ethyl acetate extract (EARP) passed this screening step and we thus prioritized it for dose dilution assays at extract concentrations of 0–240 μg/ml (Fig. 2A) and 10–0.5 μg/ml for the positive control (Supplementary Fig. 1) against HeLa to allow estimation of IC_{50} and extract concentrations of 0–800 μg/ml (Figs. 2B) and 100–1.5625 μg/ml for the positive control (Supplementary Fig. 2) against Vero cells to allow estimation of CC_{50}. EARP had an IC_{50} concentration of 77.87 ± 2.38 μg/ml and a CC_{50} value of 342.64 ± 3.35 μg/ml while doxorubicin hydrochloride (the positive control) had an IC_{50} value of 1.45 ± 0.20 μg/ml and a CC_{50} value of 4.52 ± 1.24 μg/ml compared to the negative control (Table 3). These findings show that the EARP extract suppressed cell growth in a way that was dose-dependent.

We further estimated the selectivity index (SI) to assess the selective toxicity of EARP towards cervical cancer cells compared to non-cancerous cells. A selectivity index of ≥1 indicates that the extract is selective for cancer cells when compared to non-cancerous cells [30]. The selectivity index of EARP was calculated to be 4.40 and 3.12 for the positive control (doxorubicin hydrochloride), indicating a strong selectivity of the extract against cancer cells (Table 3).

3.3. Phenotypic examination of the cytotoxic effects of EARP on cervical cancer cells

We sought to show the cytotoxicity of EARP in HeLa cells after 48 h of treatment at different concentrations, along with the negative and positive controls (Fig. 3). The results demonstrated that the higher the concentration of the extract the higher the cytotoxic effect exhibited and vice versa in comparison to the negative control. Furthermore, HeLa cells exposed to varying concentrations of EARP exhibited atypical morphology with cellular shrinkage, losing their sphere-shape and also suffering surface detachment, which is an indication of extracts cytotoxic effects.

Table 2
Percentage yield of *R. prinoides* extracts.

Plant weight plant	Crude		Hexane		Ethyl acetate		Water	
800g	**Weight**	**% Yield**	**Weight**	**% Yield**	**Weight**	**% Yield**	**Weight**	**% Yield**
	11.1g	**1.39**	4.1g	**0.5**	3.1g	**0.39**	3.1g	**0.39**
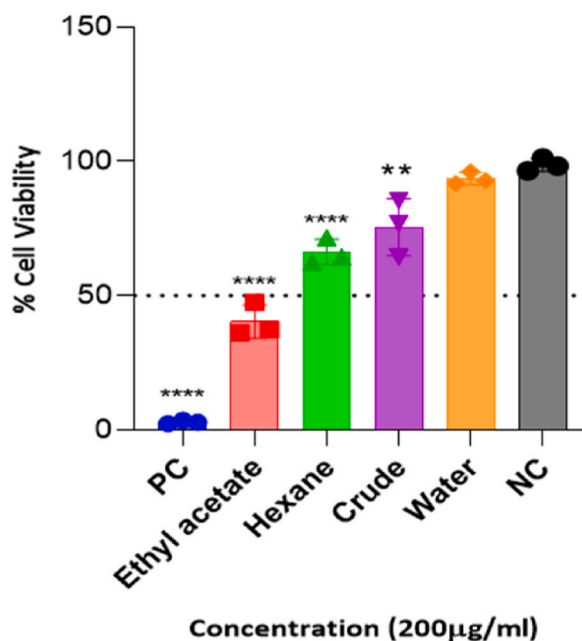
Fig. 1. Screening of the water-, crude-, hexane- and ethyl acetate extract extracts of *R. prinoides* at 200 µg/ml in HeLa cells. **p < 0.01, ****p < 0.0001 vs the negative control (0.4 % DMSO, NC). Doxorubicin hydrochloride was used as the positive control (PC). Data is represented as mean ± SD of three distinct experiments conducted in triplicate.
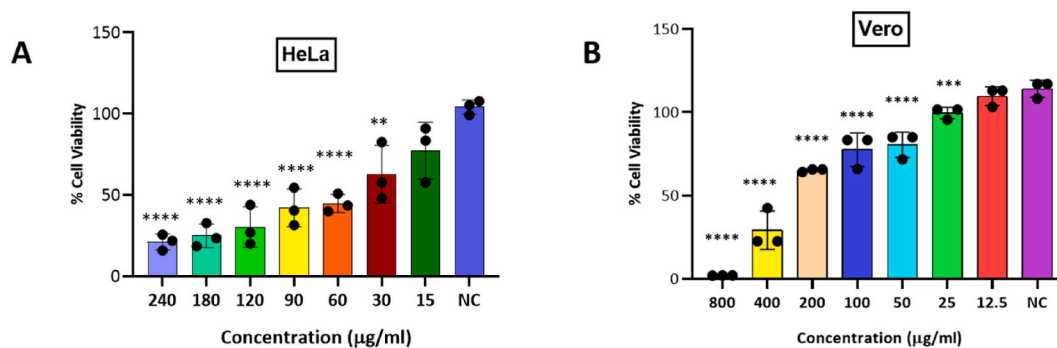
Fig. 2. *In vitro* anti-proliferation effects of EARP in cervical cancer cells (HeLa) and Vero cells. A- Dose-dependent effect of EARP on HeLa cells. B- Dose dependent effect of EARP on Vero cells. **p < 0.01, ***p < 0.001, ****p < 0.0001 vs the negative control (0.4 % DMSO, NC). Data is represented as mean ± SD of three distinct experiments conducted using three technical replicates.

Table 3
Table of IC_{50}, CC_{50} and Selectivity Index of EARP and the positive control.

	IC_{50} (µg/ml)	CC_{50} (µg/ml)	Selectivity Index (SI)
EARP	77.87 ± 2.38	342.64 ± 3.35	4.40
Doxorubicin hydrochloride (PC)	1.45 ± 0.20	4.52 ± 1.24	3.12

3.4. EARP's effect on the limiting migration and invasion

We utilized the *in vitro* wound healing assay to assess EARP's effectiveness to prevent cervical cancer cell migration, a marker of cancer spread. HeLa cells got an artificial wound and the percentage wound closure was noted after 0, 24 and 48 h. The results indicated that unlike the cells treated with the negative control, EARP successfully impeded the migration of HeLa cells at IC_{50}, IC_{25} and $IC_{12.5}$ concentrations in a manner that was dependent on the dose and time of the treatment (Fig. 4). The IC_{50} concentration showed the highest inhibitory effect to migration followed by the IC_{25} while $IC_{12.5}$ had the lowest inhibitory effect over time.
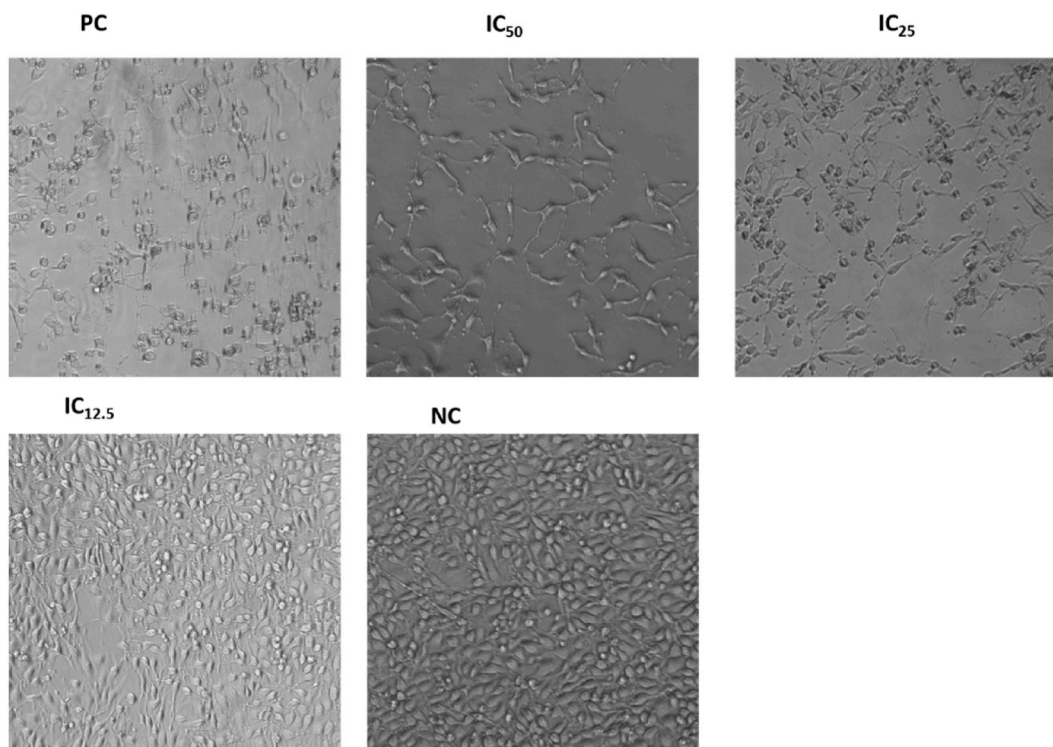
Fig. 3. Phenotypic evidence of cytotoxicity of EARP at different concentrations in HeLa cells at ×200 magnification; NC- negative control (0.4 % DMSO) and PC-positive control.
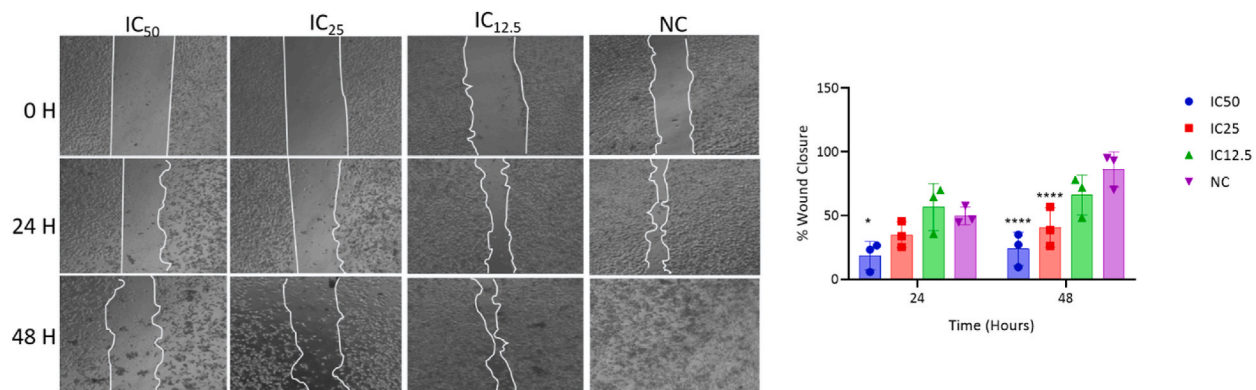
Fig. 4. Wound healing analysis of EARP in HeLa cells recorded at 0, 24 and 48 h at IC_{50}, IC_{25} and $IC_{12.5}$ concentrations with a graph showing the % wound closure at 24 and 48 h relative to 0 h on the right, captured at ×200 magnification. *p < 0.05, ****p < 0.0001 vs the negative control (0.4 % DMSO, NC). Data is represented as mean ± SD of three distinct experiments using three technical replicates.

3.5. The effect EARP on the cell cycle

We used flow cytometric analysis to evaluate the extent to which EARP induced restriction of the cell cycle of HeLa cells. We determined that the treatment at IC_{50} and IC_{25} concentrations of EARP for 48 h caused restriction of the cell cycle at the S phase (Fig. 5). The percentage number of HeLa cells at G2/M phase after treatment with IC_{50} (0.710 ± 1.230) and IC_{25} (3.743 ± 4.353) concentrations of EARP was notably less than those in the negative control group (31.733 ± 2.779).

3.6. Secondary metabolites in EARP

To evaluate the secondary metabolites present in EARP, we conducted qualitative color change based screening tests. Secondary metabolites are the classes of compounds that are present and that are linked to activity of that plant. We found that glycosides, tannins
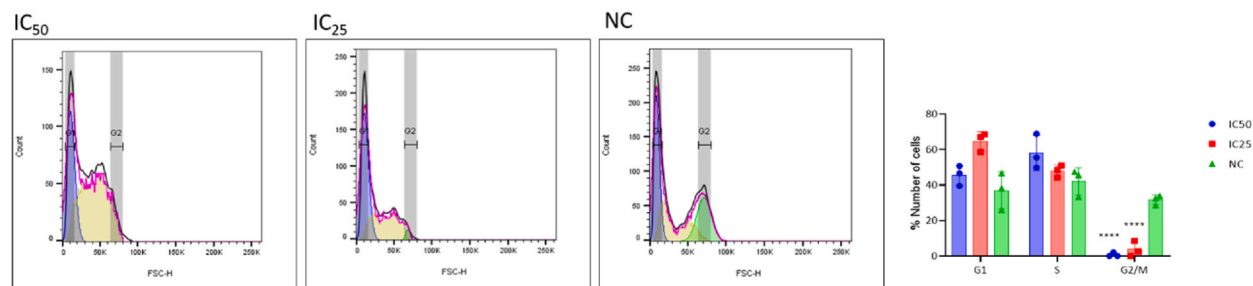
Fig. 5. Flow cytometric analysis of EARP at IC_{50} and IC_{25} concentrations relative to the negative control after treatment for 48 h in HeLa cells. The graphs show that majority of the cells in the treated groups accumulated in the S phase compared to cells in the negative control group that were able to move to the G2/M phase. Up to 10,000 cells were evaluated in every sample. ****$P < 0.0001$ vs NC. Data is represented as mean $\pm$ SD in triplicate.

and phenols were the most abundant secondary metabolites in EARP. Terpenoids and alkaloids, were also present. We could not detect any flavonoids and saponins (Table 4).

3.7. Gas chromatography/mass spectrometry analysis of EARP

We carried out GC/MS analysis to qualitatively determine the compounds present in EARP that can partly be linked to its bioactivity. We identified 12 compounds in EARP (Supplementary Fig. 3). We found that the most abundant compounds were 3-Amino-4-(4-ethoxy-phenylamino)-benzoic acid (59 %) and 3-Ethoxy-4-methoxybenzaldehyde (10 %) (Table 5).

3.8. Results on in silico studies

3.8.1. ADMET properties of the compounds in EARP

Out of the 12 compounds we identified by GC/MS we only selected 7 for downstream experiments as the others failed to meet the criteria for drug-likeness which included not violating more than one of the five Lipinski rules, not having the capacity to cross the blood-brain barrier, not being an inhibitor of cytochrome P450 enzymes and not having a topological surface area more than 140 Å^2. We excluded 3-Amino-4-(4-ethoxy-phenylamino)-benzoic acid as the canonical smile could not be generated. We selected the 7 compounds that met the criteria; 8-Hexylpentadecane, Eicosane, 9-methylnonadecane, 2-methyloctacosane, Squalene, Olean-12-en-3.beta.-ol, acetate and 3,3a,6,6-tetramethyl-4,5,5a,7,8,9-hexahydro-1H-cyclopenta[i]indene (Table 6).

We then assessed the toxicity profile of the compounds. The total clearance is a combination of the hepatic clearance and renal clearance of a compound and it gives the amount of dosage rate for steady concentrations of a drug. It is given as log (ml/min/kg). AMES toxicity is a test which determines whether a compound has the potential to be carcinogenic or not, we found that none of the compounds had AMES toxicity which implies that they cannot induce carcinogenesis. The Max tolerated dose gives an indication of the maximum dose that is tolerated in human beings, for a compound a maximum tolerated dose $\leq$0.477 Log (mg/kg/day) is considered low while a value $\geq$ 0.477 is considered high, we found that only 3-ethoxy-4-methoxybenzaldehyde had a high max tolerated dose. Hepatotoxicity is a measure of the likelihood of a compound to cause drug-induced liver injury, we found that only 2',4'-Dihydroxypropiophenone showed that likelihood. Inhibition of potassium channels encoded by the hERG gene (human ethyl-a-go-go gene) may lead to the development of long QT syndrome which can lead to a heart attack, we found that none of the compounds inhibited hERG I, however, only 3-ethoxy-4-methoxybenzaldehyde, 4-tert-Butylphenyl acetate, 2',4'-Dihydroxypropiophenone, 3,3a,6,6-tetramethyl-4,5,5a,7,8,9-hexahydro-1H-cyclopenta[i]indene did not inhibit hERG II (Supplementary Table 2).

3.8.2. Generation of EARP targets of the prioritized putative compounds and cervical cancer

We retrieved compound target genes from EARP from three databases namely the SEA database (37), Swiss Target Prediction

Table 4
Phytochemical profile of EARP.

	EARP
Alkaloids	++
Saponins	-
Flavonoids	-
Terpenoids	++
Glycosides	++++
Tannins	++++
Phenols	++++

++++ = highly abundant, +++ = abundant,
++ = present, and - = undetectable quantities.

Table 5
The compounds present in EARP identified through GC/MS analysis.

Peak Number	Retention Time	% Area	Name	Molecular formula	Molecular weight (g/mol)	Compound class
1	15.687	10.38	3-Ethoxy-4-methoxybenzaldehyde	$C_{10}H_{12}O_3$	180.20	Benzaldehyde
2	15.815	1.49	4-tert-Butylphenyl acetate	$C_{12}H_{16}O_2$	192.25	Phenol
3	17.174	5.32	2′,4′-Dihydroxypropiophenone	$C_9H_{10}O_3$	166.17	Phenol
4	20.166	1.88	2-(3-Phenyl-piperidin-1-yl)-ethylamine	$C_{13}H_{20}N_2$	204.31	Phenethylamine
5	20.697	1.62	Eicosane	$C_{26}H_{54}$	366.7	Hydrocarbon
6	21.601	1.6	8-Hexylpentadecane	$C_{21}H_{44}$	296.6	Hydrocarbon
7	22.547	58.74	3-Amino-4-(4-ethoxy-phenylamino)-benzoic acid	$C_{15}H_{16}N_2O_3$	272	Methyl benzoic acid
8	24.101	1.67	9-Methylnonadecane	$C_{20}H_{42}$	282.5	Methylated hydrocarbon
9	24.95	1.63	2-methyloctacosane	$C_{29}H_{60}$	408.8	Methylated hydrocarbon
10	26.165	2.86	Squalene	$C_{30}H_{50}$	410.7	Triterpenoid
11	27.731	3.89	Olean-12-en-3.beta.-ol, acetate	$C_{32}H_{52}O_2$	468.8	Triterpenoid
12	29.721	6.49	3,3a,6,6-tetramethyl-4,5,5a,7,8,9-hexahydro-1H-cyclopenta[i]indene	$C_{16}H_{26}$	218.38	Pyrimidine derivative

Table 6
Physio-chemical properties of EARP compounds.

Compounds	Molecular weight (g/mol)	Hydrogen acceptors	Hydrogen donors	MOL LOG P	TPSA (Å²)	Lipinski's rule violation	Blood-brain barrier
Threshold	≤500	≤10	≤5	≤5	≤140	Yes/No	Yes/No
EARP1	180.2	3	0	1.13	35.53	No	Yes
EARP2	192.25	2	0	3.13	26.3	No	Yes
EARP3	166.17	3	2	0.83	57.53	No	Yes
EARP4	204.31	2	1	2.02	29.26	No	Yes
EARP5[a]	366.71	0	0	8.66	0	Yes,1	No
EARP6[a]	296.57	0	0	7.6	0	Yes,1	No
EARP7[a]	282.55	0	0	7.38	0	Yes,1	No
EARP8[a]	408.79	0	0	9.25	0	Yes,1	No
EARP9[a]	410.72	0	0	7.93	0	Yes,1	No
EARP10[a]	468.75	2	0	7.08	0	Yes,1	No
EARP11[a]	218.38	0	0	5.9	0	Yes,1	No

1 TPSA (Topological Surface Area Å²), MolLogP (Octanol/Water) Lipophilicity, BBB (Blood Brain Barrier) EARP (Ethyl acetate extract of *R. prinoides*), EARP1 (3-ethoxy-4-methoxybenzaldehyde), EARP2 (4-tert-Butylphenyl acetate), EARP3 (1-(2,4-dihydroxyphenyl)propan-1-one), EARP4 (2-(3-phenylpiperidin-1-yl)ethanamine), EARP5 (Eicosane), EARP6 (8-Hexylpentadecane), EARP7 (9-methylnonadecane), EARP8 (2-methyloctacosane), EARP9 (Squalene), EARP10 (Olean-12-en-3.beta.-ol, acetate), EARP11 (3,3a,6,6-tetramethyl-4,5,5a,7,8,9-hexahydro-1H-cyclopenta[i]indene).
[a] Compounds that showed good drug-likeness.

database (265) and the Super-PRED database (340). 636 genes were retained after the gene targets from the three databases were combined into a single column and the duplicates eliminated. We retrieved cervical cancer genes from GeneCards (6406), OMIM (120), Dis GENET (1817) and NCBI (1759) databases, we compiled the target genes into a single column and duplicates were deleted retaining 6937 targets genes. We then used an online Venn diagram generator to find the common genes between the genes retrieved from cervical cancer and those from our compound targets (Fig. 6A). We found 246 common genes (Supplementary sheet) from which we generated a network consisting of 246 nodes and 3508 number of edges with an estimated mean degree in the nodes of 28.6 and an estimated mean local clustering coefficient of 0.518. We found that the protein-protein network exhibited a substantially higher number of interactions than anticipated, with a protein-protein interaction enrichment P value of <1.0e- 16, alluding to strong biological interconnectedness among its constituent genes (Supplementary Fig. 4).

3.8.3. Identification of top hub genes

We loaded the 246 genes into STRING database where a PPI network was constructed and then exported the network to the Cytoscape application version 3.10.2 for visualization of the protein-compound-target network (Fig. 6B) and using the Cytohubba plugin we generated the top 30 hub genes based on five topological analysis methods; the degree, eccentricity, betweenness, closeness and maximal clique centrality (MCC) (Fig. 6C), and generated a gene-compound network of the top 30 genes and the compounds used for docking (Fig. 6D).

3.8.4. GO and KEGG enrichment analysis

We found that the key genes (246) from EARP were enriched in 2029 GO (Gene Ontology) terms; 1733 GO-terms were notably enriched in biological processes, 198 GO-terms were notably enriched in molecular functions and 98 GO-terms were significantly enriched in cellular components, (p < 0.05). The key GO-terms in terms of cellular components, biological processes, and molecular
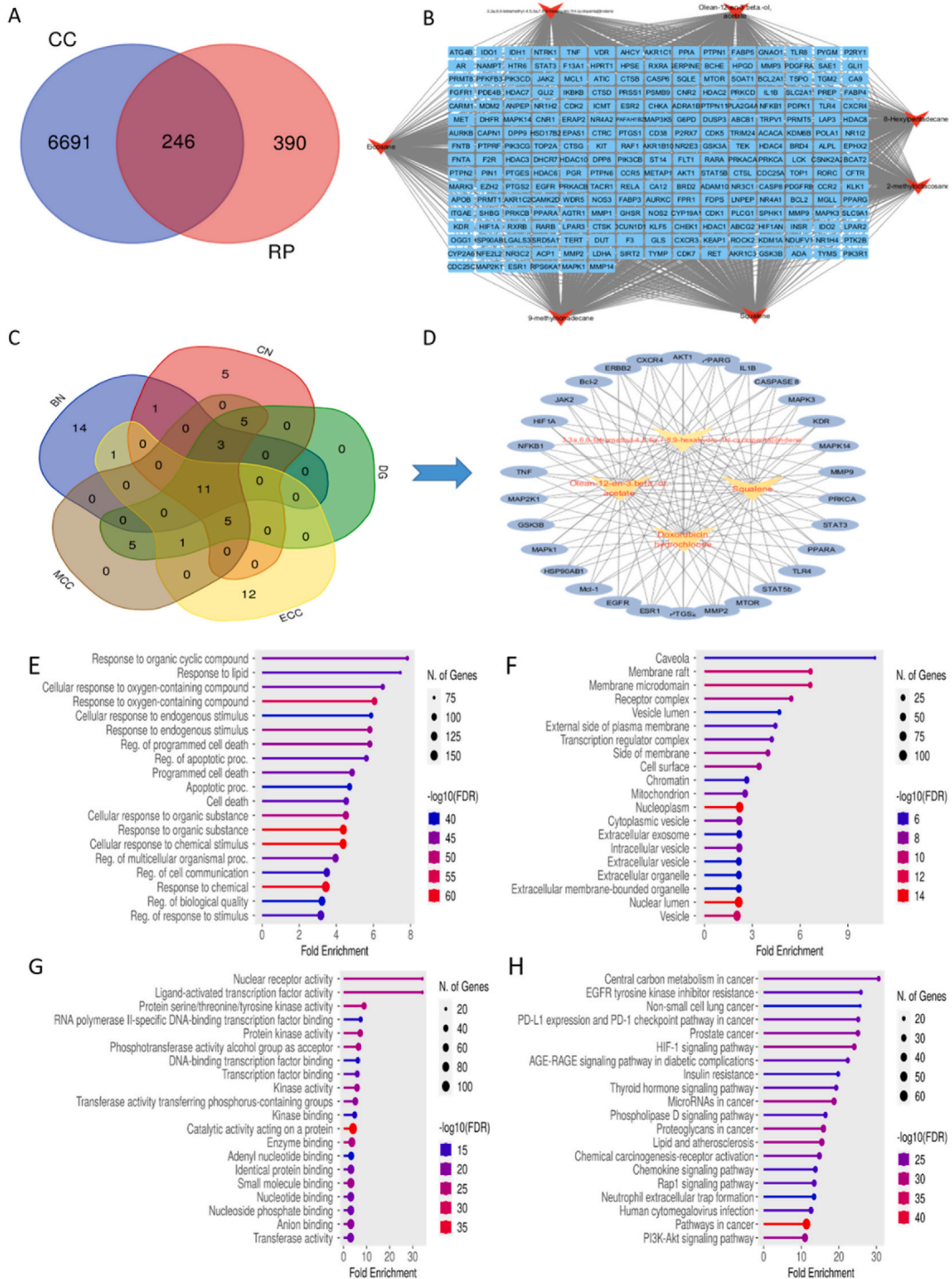
(caption on next page)

Fig. 6. *In silico* and network pharmacological analysis of the compounds and gene targets of EARP. A- Venn illustration of the common targets of EARP and cervical cancer; RP- *Rhamnus prinoides*, CC-cervical cancer B- Illustration of a generated compound-target network by Cytoscape. C-Venn illustration of the topmost 30 genes gotten from the Cytohubba plug in Cytoscape using BN (Betweenness), MCC (Maximal Clique Centrality), ECC (Eccentricity), DG (Degree) and CN (Closeness) parameters. D- Compound-target network of the top 30 hub genes and the selected compounds for molecular docking. E-GO enrichment assessment of the common gene targets of the compounds in EARP in biological processes, F- Cellular Component, G-Molecular Function. The bubble size depends on the number of genes associated the process, function or component where a larger bubble represents more genes and vice versa. The color shows the adjusted P-value for the pathway analysis, with the more red the bubble, the higher the FDR and vice versa. H- 6 KEGG pathway enrichment analysis. The KEGG terms are shown on the left vertical axis while the Log P values are shown on horizontal axis. On the right is the false discovery rate (FDR) which is indicated by the color intensity with the darker red color indicating a higher FDR. The bubble size corresponds to the number of genes associated with the pathway with a bigger bubble indicating a larger pool of genes compared to small bubbles on the plot. (For interpretation of the references to color in this figure legend, the reader is referred to the Web version of this article.)

functions are shown below (Fig. 6E–G). The x-axis is representative of the number of enrichments while the y-axis represents the enriched categories in each group. The order of importance is from top to bottom and it is ranked by –log10 (False Discovery Rate). GO analysis established that in biological processes the key genes play a role in responses to organic cyclic compounds, responses to lipid and cellular responses to oxygen-containing compounds respectively in order of the number of genes. In cellular components the main enrichment was in the caveola, membrane raft and membrane micro-domain respectively while in the molecular functions, the enrichment was in the nuclear receptor activity, ligand-activated transcriptional factor activity and protein serine/threonine/tyrosine kinase activity. 196 pathways were notably enriched in the KEGG pathway, with the top 20 pathways being displayed (-LogP) (Fig. 6H).

3.9. Molecular docking analysis

We considered the 30 top hub genes receptors and the 7 compounds ligands for molecular docking. We only utilized three compounds, 3,3a,6,6-tetramethyl-4,5,5a,7,8,9-hexahydro-1H-cyclopenta[i]indene, Olean-12-en-3.beta.-ol, acetate and Squalene, for docking as the other 4 compounds were too flexible. We also docked the positive control, doxorubicin hydrochloride, against the proteins. We found that all the compounds had a binding affinity ≤ -4 (Fig. 7A and Supplementary Table 1). Most of the interactions between the ligands and the proteins that had a binding affinity of ≤ -7.5 were hydrophobic in nature; π- Alkyl, π-sigma and van der Waals forces (Table 7). We selected the best docking results for visualization using BIOVIA Discovery Studio software 2021 (Fig. 7B).
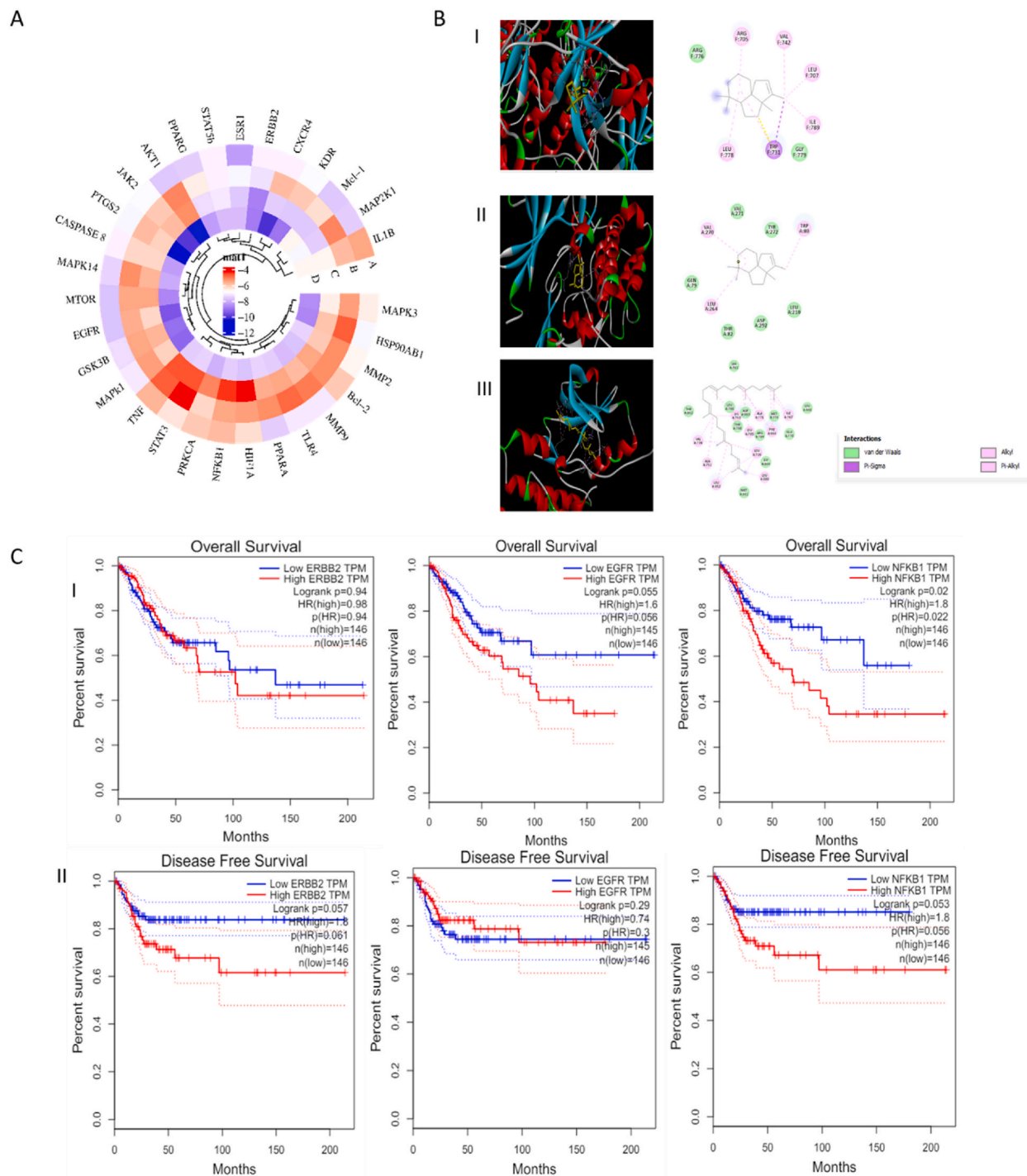
3.10. Survival analysis

We conducted survival analysis of EGFR and Er-b-B2 which were among the top 30 hub genes identified through network pharmacology using GEPIA. We also analyzed NF-κB expression for its role in enhancing migration of cervical cancer cells. The analysis of survival showed important differences in the overall survival between high expression groups of EGFR and NF-κB genes and those of low expression groups with p-values of 0.02 and 0.055 respectively (Fig. 7CI). There was also an important difference in the disease free survival in groups with high expression and low expression of NF-κB and Er-b-B2 with p-values of 0.057 and 0.053 respectively (Fig. 7CII).

3.11. EARP affects the mRNA expression of genes related to cervical cancer

We selected the genes with the lowest binding affinities as well as those linked to the progression of cervical cancer such as tumor protein 53 and Bax protein to validate their mRNA expression levels *in vitro* through RT-qPCR. GAPDH and β-actin were used as internal references. EGFR, Er-b-B2, Bcl-2 and NF-κB were among the top 30 hub genes identified through network pharmacology and their activity was validated using molecular docking and found to be ≤ -5. The method of $2^{\Delta\Delta Ct}$ method was utilized to calculate the mRNA expression of the genes. AKT1 (0.149 ± 0.061), Bcl-2 (0.284 ± 0.270), NF-κB (0.144 ± 0.120) and Er-b-B2 (0.280 ± 0.262) mRNA levels were significantly downregulated in comparison to the negative control cells with p values of $p = 0.0036$, $p = 0.0036$, $p = 0.0009$ and $p = 0.0035$ respectively while Bax (3.285 ± 1.407) and p53 (3.273 ± 0.728) were significantly upregulated with $p = 0.0389$ and $p = 0.0397$ values respectively. The difference ($p = 0.3248$) between the mRNA expression of EGFR (0.504 ± 0.006) and that of the negative control cells, however was not significant (Fig. 8).

4. Discussion

Cervical cancer is still a significant burden among gynecological diseases in women, with the worldwide mortality burden being heaviest in Eastern Africa [31]. Radiation therapy, chemotherapy and surgery are the most employed regimens [32]. Chemotherapy, which is the most common treatment, is encumbered with limitations such as severe side effects and chemo-resistance, while surgery is laden with tumor recurrence and metastasis. Novel therapeutic agents that are less toxic are therefore needed. Plant secondary metabolites and their bioactive constituents can be essential in cervical cancer management and therapy due to the myriad of bioactive compounds that they contain, such as polyphenols, tannins, flavonoids, glycosides and many more, which have been shown to have anti-cancer activities [33]. Today, several potent anti-cancer drugs are used from plant origins such as vincristine, taxol, etoposide and

Fig. 7. *In silico* and survival analysis of the genes affected by the compounds in EARP. A- Heat map of the docking scores of the compounds in EARP as well as the positive control, doxorubicin hydrochloride and their protein targets. Key- A- 3,3a,6,6-tetramethyl-4,5,5a,7,8,9-hexahydro-1H-cyclopenta[i]indene, B- Olean-12-en-3.beta.-ol, acetate, C- Squalene and D- Doxorubicin hydrochloride. B- 3D diagrams of ligand-protein poses of docked genes and 2D illustrations of ligand-protein interactions respectively generated from Discovery Studio 2021.Key: I-EGFR+ 3,3a,6,6-tetramethyl-4,5,5a,7,8,9-hexahydro-1H-cyclopenta[i]indene, II- AKT1+ 3,3a,6,6-tetramethyl-4,5,5a,7,8,9-hexahydro-1H-cyclopenta[i]indene,III- Er-b-B2+Squalene. C- Target genes survival analysis gotten from the GEPIA database. I-Overall survival analysis of Er-b-B2, EGFR and NF-κB genes respectively; II- Disease free survival analysis of Er-b-B2, EGFR and NF-κB genes respectively.

Table 7
Molecular docking interactions

COMPOUND	PDB CODE	PDB ID	NAME	BINDING AFFINITY (KJ/ MOL)	BOND TYPE	AMINO ACIDS
3,3a,6,6-tetramethyl- 4,5,5a,7,8,9-hexahydro- 1H-cyclopenta [i] indene	EGFR	5gty	Epidermal Growth Factor Receptor	−7.8	Van der Waal forces	ARG 776 GLY 779
					π- sigma	TRP 731
					π- Alkyl/ Alkyl	LEU 778 LEU 707 ARG 705 VAL 742 ILE 789
	AKT-1	3o96	AKT Serine/Threonine Kinase 1	−7.7	Van der Waal forces	VAL 271 TRP 272 LEU 210 ASP 292 THR 82 GLN 79
					π- sigma	TRP 80
					π- Alkyl/ Alkyl	VAL 270 LEU 264 LEU 525 LEU 346
Squalene	Er-b-B2	7 pcd	erb-b2 Avian Erythroblastic Leukemia Viral Oncogene Homolog 2	−8.9	Van der Waal forces	SER 783 GLY 804 THR 852 MET 801 ARG 784 LEU 796 ASP 863 LEU 866 MET 774 GLU 770 THR 798
					π- Alkyl/ Alkyl	VAL 734 ALA 751 LEU 852 LEU 800 LYS 753 LEU 785 ALA 771 PHE 854 ILE 767
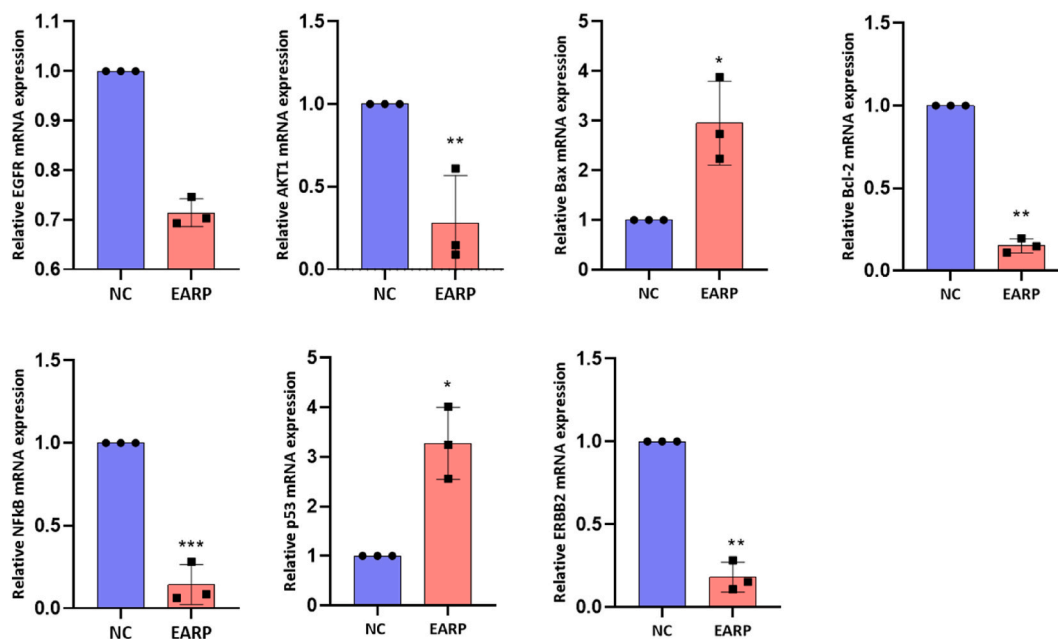
Fig. 8. The mRNA expression of EGFR, AKT1, Bax, Bcl-2, NF-κB, Er-b-B2 and p53 genes using RT-qPCR in HeLa cells after treatment with EARP for 48 h *p < 0.05, **p < 0.01 and ***p < 0.001 vs negative control (0.4 % DMSO, NC) generated using one-way ANOVA in Graph pad prism 8.0.2. Data is presented as mean ± SD conducted in triplicate.

topotecan. The National Cancer Institute has gathered over 30,000 samples from plants in over 20 nations thus far, and it has examined over 100,000 extracts for potential anti-cancer properties [34]. We sought to investigate the *R. prinoides* extracts' cytotoxicity using HeLa cells and non-cancerous Vero cells, to investigate whether they influenced the migration of the cells, to determine the compounds in the active extract through GC/MS analysis that could be partly responsible for their bioactivity and the genes these compounds potentially interacted with and to determine the interaction between the genes and the compounds through molecular docking and RT-qPCR.

Extraction of secondary metabolites is a process by which, as the solvent flows into the cell, the protoplasm swells and the compounds in the cell dissolve in the solvent. The compounds dissolve according to their solubility in the solvent, which depends on the solvent polarity. Solvents dissolve the phytochemicals that share their polarity [35]. We used solvents with increasing polarity to compartmentalize the extracts according to their polarity. The percentage yield of an extract represents the abundance of the extract in the plant part used for the study. Various factors contribute to an extracts' percentage yield, including the period the solvent and plant

parts come into contact, as more extended contact periods result in higher extracts [36]. We repeated the extraction procedure several times until a color change was observed to extract the phytochemicals exhaustively. The crude extract yielded the highest percentage of 1.06 %, while the ethyl acetate fraction yielded the lowest percentage of 0.39 % (Table 2). These results are similar to a study by Rashid et al. 2022, which showed that the ethyl acetate extract of *Aloysia citrodora* had the second lowest percentage yield after the essential oils [37].

The MTT assay is a reliable and sensitive measure of cell viability. It runs on the basis that the amount of the dark, insoluble purple formazan product produced is directly tied to the number of live cells in the well and is produced by the mitochondrial dehydrogenase enzymes. As demonstrated in Fig. 1, EARP was the most active extract fraction against cervical cancer cells. It showed moderate activity according to the criteria in Kuete et al., 2013, that is, a plant extract is considered to have high activity if it has an IC_{50} value less than 50 µg/ml, moderate activity if it has an IC_{50} value between 50 µg/ml and 200 µg/ml, low activity if it has an IC_{50} value between 200 µg/ml and 1000 µg/ml and no activity if it has an IC_{50} value greater than 1000 µg/ml [38]. EARP was then assessed for selective anti-proliferative activity and was shown (Fig. 2A and B) to have selective anti-proliferative activity against HeLa cells, with the IC_{50} of 77.87 µg/ml being significantly lower than the CC_{50} in Vero cells (342.63 µg/ml) by a fold of 4.40 which is interestingly higher than the selectivity of the positive control (doxorubicin hydrochloride) which had a selectivity index of 3.12 (Table 3). The effects of the extracts can also be visualized phenotypically when compared with cells treated with the negative control (0.4 % DMSO) (Fig. 3) as the shape of the cells changes from long and elongated to small round cells. The selectivity of EARP is consistent with a study on the anti-proliferation activity of flavonoids from *Rhamnus davurica* against human colon carcinoma and gastric carcinoma (24.96 and 89.53 µg/ml respectively) being higher than normal hepatic cells, L-O2 (229.19 µg/ml) by a factor of 7.64 and 2.55 respectively [39].

Cancer metastasis is a huge cause of cancer-related mortality for many cancer patients, more so for cervical cancer patients in late stages [32,40,41]. Prevention of metastasis, is therefore, an essential tool in improving the chances of survival and plant extracts are shown to have anti-metastatic potential [42]. We assessed the potential of EARP in inhibiting metastasis using the *in vitro* wound healing migration assay. The results (Fig. 4) revealed that EARP inhibited migration of HeLa cells dose- and time-dependently, with the IC_{50} concentration having the highest inhibitory effect, followed by the IC_{25} concentration after 24 and 48 h. A study of methanolic neem extracts showed similar anti-migratory effects on cervical cancer cells at 30 µg/ml, 20 µg/ml and 10 µg/ml [20]. NF-κB is a transcriptional factor that has been linked to invasion and migration in cervical cancer by facilitating the transcription of downstream genes that promote migration, vascularization and proliferation [43]. We assessed the mRNA levels of NF-κB in this study after treatment with EARP at the IC_{50} concentration and the levels were downregulated by a factor of 0.144 compared with the cells treated with 0.4 % DMSO (Fig. 8). Additionally, survival analysis revealed that high expression of the NF-κB gene (Fig. 7C) in cervical cancer patients is linked to lower general survival and lower disease-free survival of cervical cancer patients. These findings indicate that EARP is effective in limiting cervical cancer cells' migration ability and improving patient survival.

The cell cycle is the tool cells use to control whether a cell is quiescence or proliferative. It plays a paramount role in the conversion of cells to malignancy. Checkpoints in the cell cycle control its progression, preventing the cells from moving on to the next phase if there is damage to their DNA [44,45]. In this study, we observed the restriction of the cell cycle induction at the S phase as there was an increased number of cells in the S phase at IC_{50} and IC_{25} concentrations with fewer cells moving to the G2/M phase (Fig. 5). Since the progression through the checkpoints, especially the S phase is moderated through DNA synthesis, the increased number of cells in the S phase after EARP treatment with the IC_{50} and IC_{25} concentrations could be indicative of DNA damage caused by the extracts preventing the damaged DNA from moving on to mitosis and arresting the cells at the S phase. Similar results were shown in HeLa cells exposed to extracts from *Allium atroviolaceum* and in HeLa cells exposed to varying concentrations of methanolic neem extract [20,46]. When DNA damage occurs, tumor suppressor protein 53 is known to restrict the cell cycle and cause apoptosis [47]. Tumor suppressor protein 53 is known to have mutations in many human cancers (>50 %) [48]. We tested the mRNA levels of tumor protein 53 in cells treated with EARP and compared them to those treated with the negative control. The results showed that in EARP, tumor protein 53 levels were upregulated 3.273 times (Fig. 8). We found that in addition to increased expression of p53 there was also a corresponding increase in mRNA levels of Bax and reduction of the mRNA levels of Bcl-2, by a fold change of 3.285 and 0.284 relative to the cells that received the negative control (Fig. 8). EARP may cause apoptosis through increased transcription of p53 and inhibition of transcription of Bcl-2 (Fig. 9). Similarly, HeLa cells treated with *Allium atroviolaceum* extracts showed increased p53 mRNA levels with decreased mRNA levels of Bcl-2 [46]. Additionally, *in silico* evaluation of the interaction between Mcl-1, which is an anti-apoptotic protein that binds to Bax and Bak proteins, inhibiting their activation of the apoptosis cascade was evaluated and two compounds 3,3a,6,6-tetramethyl-4,5,5a,7,8,9-hexahydro-1H-cyclopenta[i]indene and squalene showed good binding affinity, −7.7 kJ/mol (Supplementary Table 1), to similar pockets as that on macrocyclic inhibitors of Mcl-1 independent of the BH3 binding domain [49].

The phytochemicals in the extract form the basis for all of EARP's anti-proliferation activities. Qualitatively, the most abundant classes of secondary metabolites were glycosides, tannins and phenols while alkaloids and terpenoids were present (Table 4). All these classes of phytochemicals are demonstrated to possess anti-cancer activities *in vitro* [50–54]. GC/MS analysis found that the majority of compounds identified were hydrocarbons, triterpenoids and a pyrimidine derivative (Table 5). Various triterpenoids and their derivatives have been implicated in anti-proliferation activity in cervical cancer cells *in vitro* [55–57]. Squalene, a triterpene present in EARP (Table 5) has been shown to elicit *in vitro* anti-proliferative activity in HepG2 cells (IC_{50} of 100 µg/ml) [58]. Although not as popular as other secondary metabolites, pyrimidine derivatives, are emerging as key compounds in anti-cancer therapy through various mechanisms, the most characterized being as tyrosine protein kinase inhibitors [59]. 3,3a,6,6-tetramethyl-4,5,5a,7,8,9-hexahydro-1H-cyclopenta[i]indene, which is pyrimidine derivative was identified in EARP (Table 5). Small molecule inhibitors are emerging as promising therapies for cancer, either alone or through amalgamation with current treatments. They are most promising as they provide targeted therapies and are more selective. Most of the small molecule inhibitors used currently target receptors and
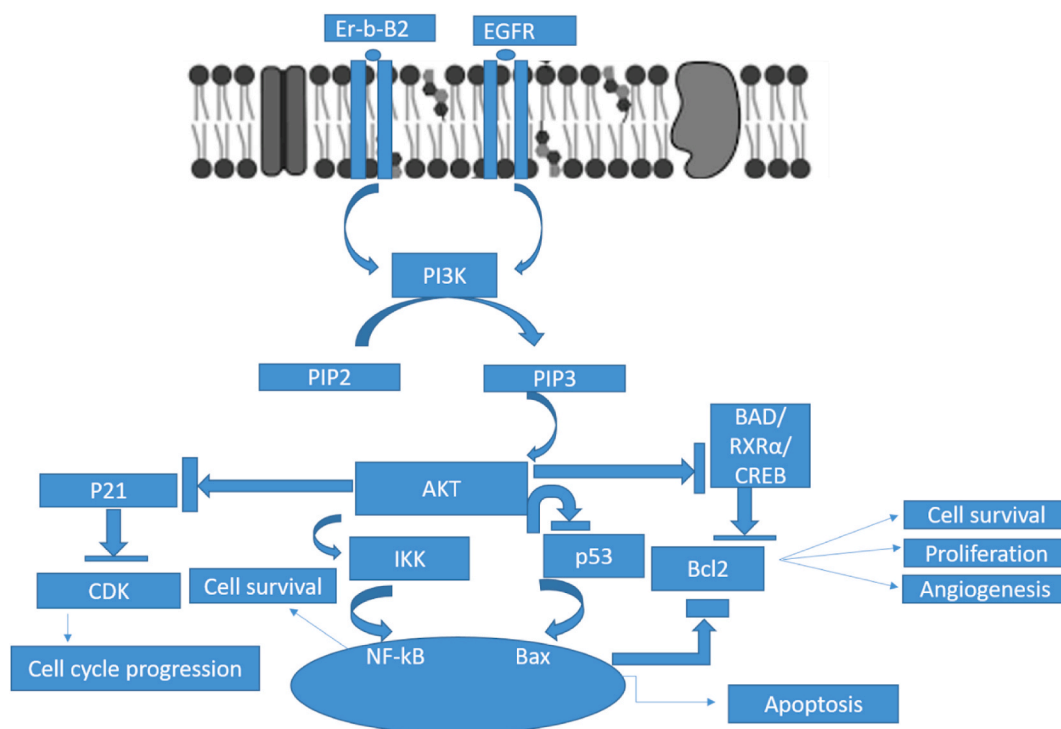
Fig. 9. Interaction of genes in the PI3K pathway and the compounds in EARP, following molecular docking analysis and validated by RT-qPCR and their consequences to cervical cancer progression.

proteins found in pathways that are key to cancer development, proliferation and migration [60]. From the analysis of gene ontology through biological pathways, molecular functions and cellular components, there are a variety of pathways in which the compounds are predicted to be involved in inhibiting the proliferation of cervical cancer cells. These include central carbon metabolism in cancer, the EGFR tyrosine inhibitor resistance, apoptosis, Ras signaling pathway, pathways in cancer and the PI3K-Akt signaling pathway (Fig. 6E–H). Common genes between cervical cancer and the compounds in EARP were evaluated and the top 30 genes based on their interactions with the network were chosen as the hub genes (Fig. 6D). The hub gene proteins were docked against the compounds and the gene proteins with the lowest docking affinity and known affiliation to cervical cancer pathways such as the PI3K-Akt pathway, cell cycle pathway and apoptosis pathway were validated using RT-qPCR. 3,3a,6,6-tetramethyl-4,5,5a,7,8,9-hexahydro-1H-cyclopenta[i] indene compound showed good binding affinity with AKT1 of -7.7 kJ/mol (Table 7) in the same position as another AKT1 inhibitor in the membrane-associated PH-out form which leaves the ATP-binding site open so that when a ligand binds to the AKT1, it cannot close and instead of becoming phosphorylated and translocating to its effector protein, it remains bound to the membrane, thus inactivating it [61,62]. Squalene showed a very good binding affinity with Er-b-B2 of -8.9 kJ/mol (Table 7), which was comparable to the binding of doxorubicin hydrochloride (-9.0 kJ/mol). The binding was similar to a covalent inhibitor's binding site, inferring similar inhibition of activity [63]. The mRNA expression analysis revealed that EARP interacts with and down-regulates the expression of members of the PI3K-AKT signaling cascade. This cascade has been linked to proliferation, invasion and metastasis of cancer cells. The down-regulation of m-RNA expression of these proteins can be a mechanism by which EARP exhibits the anti-proliferative, cell-cycle arrest induction and migration-limiting properties shown (Fig. 9) [64,65]. AKT1 and Er-b-B2 mRNA levels were down-regulated compared to the negative control by a fold change of 0.149 and 0.280, respectively (Fig. 8). The survival analysis revealed that high expression of EGFR (Fig. 7C) and high expression of Er-b-B2 (Fig. 7C) is associated with lower general survival and lower disease-free survival of patients with cervical cancer when compared to low expression of the genes. EARP was shown to downregulate the expression of Er-b-B2 gene which can increase the survival prediction in cervical cancer cases. The foundation for determining the mechanisms by which EARP prevents cervical cancer from proliferating and spreading has been established by this study, underscoring the importance of these findings in cancer research and treatment.

5. Conclusion

We used various methods to assess and elucidate the mechanisms through which EARP inhibits cervical cancer proliferation and metastasis. The results show the multi-faceted nature of EARP in its inhibitory activity from impeding the proliferation of cervical cancer cells, inhibiting migration and invasion of cervical cancer cells, which is a hallmark for cervical cancer progression and inhibiting the cell cycle progression. We also showed the interaction of various compounds in EARP with various proteins key to

cervical cancer development and progression. These results can infer plant extracts' vast and far-reaching potential in cervical cancer therapy.

Study limitations and recommendations

Due to cost constraints liquid chromatography-gas spectrometry could not be conducted on EARP which would have aided in identifying all the compounds in the extract. Western blotting for the identification of the protein expression of gene proteins with the lowest binding affinities could not be conducted. We therefore recommend the assays to be conducted for a future study. We also recommend mRNA expression of the remaining docked proteins with good binding affinities with the compounds.

Data availability statement

All the data generated and analyzed during this study is included in the published article and the supplementary materials supplied.

Statement of ethics

The go-ahead for the study was granted, by the Kenya Medical Research Institute Scientific Ethical Review Unit (KEMRI/SERU/ CTMDR/104/4466).

CRediT authorship contribution statement

Sally Wambui Kamau: Writing – review & editing, Writing – original draft, Visualization, Validation, Software, Methodology, Investigation, Formal analysis, Data curation. **Mathew Piero Ngugi:** Writing – review & editing, Supervision, Methodology, Conceptualization. **Peter Githaiga Mwitari:** Writing – review & editing, Validation, Resources, Project administration, Funding acquisition, Conceptualization. **Sospeter Ngoci Njeru:** Writing – review & editing, Validation, Supervision, Project administration, Funding acquisition, Formal analysis, Data curation, Conceptualization.

Declaration of competing interest

The authors declare that they have no known competing financial interests or personal relationships that could have appeared to influence the work reported in this paper.

Appendix A. Supplementary data

Supplementary data to this article can be found online at https://doi.org/10.1016/j.heliyon.2024.e37324.

References

[1] D.M. Ba, P. Ssentongo, J. Musa, E. Agbese, B. Diakite, C.B. Traore, et al., Prevalence and determinants of cervical cancer screening in five sub-Saharan African countries: a population-based study, Cancer Epidemiology 72 (2021) 101930, https://doi.org/10.1016/j.canep.2021.101930.

[2] S.V.S. Deo, J. Sharma, S. Kumar, GLOBOCAN 2020 report on global cancer burden: challenges and opportunities for surgical oncologists, Ann. Surg Oncol. 29 (2022) 6497–6500, https://doi.org/10.1245/s10434-022-12151-6.

[3] H. Sung, J. Ferlay, R.L. Siegel, M. Laversanne, I. Soerjomataram, A. Jemal, et al., Global cancer statistics 2020: GLOBOCAN estimates of incidence and mortality worldwide for 36 cancers in 185 countries, CA A Cancer J. Clin. 71 (2021) 209–249, https://doi.org/10.3322/caac.21660.

[4] L.W. Kivuti-Bitok, G.P. Pokhariyal, R. Abdul, G. McDonnell, An exploration of opportunities and challenges facing cervical cancer managers in Kenya, BMC Res. Notes 6 (2013) 136, https://doi.org/10.1186/1756-0500-6-136.

[5] E. Jedy-Agba, W.Y. Joko, B. Liu, N.G. Buziba, M. Borok, A. Korir, et al., Trends in cervical cancer incidence in sub-Saharan Africa, Br. J. Cancer 123 (123) (2020) 148–154, https://doi.org/10.1038/s41416-020-0831-9, 1 2020.

[6] P. Memiah, W. Mbuthia, G. Kiiru, S. Agbor, F. Odhiambo, S. Ojoo, et al., Prevalence and risk factors associated with precancerous cervical cancer lesions among HIV-infected women in resource-limited settings, AIDS Research and Treatment (2012;2012) e953743, https://doi.org/10.1155/2012/953743.

[7] A. Naeem, P. Hu, M. Yang, J. Zhang, Y. Liu, W. Zhu, et al., Natural products as anticancer agents: current status and future perspectives, Molecules 27 (2022), https://doi.org/10.3390/molecules27238367.

[8] C.V. Simoben, A. Qaseem, A.F.A. Moumbock, K.K. Telukunta, S. Günther, W. Sippl, et al., Pharmacoinformatic investigation of medicinal plants from East Africa, Molecular Informatics 39 (2020), https://doi.org/10.1002/minf.202000163.

[9] J.K. Muthee, D.W. Gakuya, J.M. Mbaria, P.G. Kareru, C.M. Mulei, F.K. Njonge, Ethnobotanical study of anthelmintic and other medicinal plants traditionally used in Loitoktok district of Kenya, J. Ethnopharmacol. 135 (2011) 15–21, https://doi.org/10.1016/j.jep.2011.02.005.

[10] G. Nigussie, M. Alemu, F. Ibrahim, Y. Werede, M. Tegegn, S. Neway, et al., Phytochemicals, traditional uses and pharmacological activity of *Rhamnus prinoides*: a review, International Journal of Secondary Metabolite 8 (2021) 136–151, https://doi.org/10.21448/ijsm.833554.

[11] G. Nigussie, H. Melak, M. Endale, Traditional medicinal uses, phytochemicals, and pharmacological activities of genus *Rhamnus*: a review, Journal of the Turkish Chemical Society, Section A: Chemistry 8 (2021) 899–932, https://doi.org/10.18596/jotcsa.929188.

[12] G.N. Njoroge, R.W. Bussmann, Traditional management of ear, nose and throat (ENT) diseases in Central Kenya, J. Ethnobiol. Ethnomed. 2 (2006) 54, https://doi.org/10.1186/1746-4269-2-54.

[13] Y. Molla, T. Nedi, G. Tadesse, H. Alemayehu, W. Shibeshi, Evaluation of the in vitro antibacterial activity of the solvent fractions of the leaves of *Rhamnus prinoides* L'Herit (Rhamnaceae) against pathogenic bacteria, BMC Compl. Alternative Med. 16 (2016) 1–9, https://doi.org/10.1186/s12906-016-1279-6.

[14] T.G. Amabye, Evaluation of phytochemical, chemical composition, antioxidant and antimicrobial screening parameters of *Rhamnus prinoides* (Gesho) available in the market of Mekelle, Tigray, Ethiopia, Natural Products Chemistry & Research 4 (2016), https://doi.org/10.4172/2329-6836.1000198.

[15] G.L. Chen, F.M. Mutie, Y.B. Xu, F.D. Saleri, G.W. Hu, M.Q. Guo, Antioxidant, anti-inflammatory activities and polyphenol profile of *Rhamnus prinoides*, Pharmaceuticals 13 (2020) 1–12, https://doi.org/10.3390/ph13040055.

[16] M. Gebru, Phytochemical and Antiplasmodial Investigation of *Rhamnus prinoides* and Kniphofia Foliosa, University of Nairobi, Thesis, 2010.

[17] M. Jepkorir, S.G. Nyanjom, S. Kamau, J. Chepng'etich, G. Kipkoech, P.G. Mwitari, In vivo anti-inflammatory activity, safety and gene expression profiles of *Carissa edulis, Withania somnifera, Prunus africana* and *Rhamnus prinoides* for potential management of rheumatoid arthritis, Scientific African 22 (2023) e01933, https://doi.org/10.1016/j.sciaf.2023.e01933.

[18] H. Yusuf, M. Fahriani, C. Murzalina, Anti proliferative and apoptotic effect of soluble ethyl acetate partition from ethanol extract of *Chromolaena Odorata* Linn leaves against Hela cervical cancer cell line, Asian Pac. J. Cancer Prev. APJCP 23 (2022) 183–189, https://doi.org/10.31557/APJCP.2022.23.1.183.

[19] O.C. Chiamah, D. Atieno, L. Karani, J. Chepng'etich, M. Osano, B. Gachie, et al., Evaluation of the antimalarial properties of *Solanum incanum* L. leaf extract fractions and its ability to downregulate delta aminolevulinate dehydratase to prevent the establishment of malaria infection, J. Ethnopharmacol. 323 (2024) 117613, https://doi.org/10.1016/j.jep.2023.117613.

[20] S. Kumar, V. Mulchandani, J.D. Sarma, Methanolic neem (*Azadirachta indica*) stem bark extract induces cell cycle arrest , apoptosis and inhibits the migration of cervical cancer cells in vitro, BMC Complementary Medicine and Therapies 7 (2022) 1–16, https://doi.org/10.1186/s12906-022-03718-7.

[21] A. Somaida, I. Tariq, G. Ambreen, A.M. Abdelsalam, A.M. Ayoub, M. Wojcik, et al., Potent cytotoxicity of four cameroonian plant extracts on different cancer cell lines, Pharmaceuticals 13 (2020) 1–19, https://doi.org/10.3390/ph13110357.

[22] I.O. Okpako, Ng'ong, F.A. a, C.M. Kyama, S.N. Njeru, Antiproliferative activity of ethyl acetate fraction of *Euphorbia ingens* against prostate cancer cell line: an *in silico* and *in vitro* analysis, Scientific African 22 (2023) e01943, https://doi.org/10.1016/j.sciaf.2023.e01943.

[23] I.O. Okpako, F.A. Ng'ong'a, M.C. Kyama, S.N. Njeru, Phytochemical screening and gas chromatography-mass spectrometry analysis of *Euphorbia ingens* organic root extract, JMPR 17 (2023) 100–105, https://doi.org/10.5897/JMPR2022.7287.

[24] S. Kim, P.A. Thiessen, E.E. Bolton, J. Chen, G. Fu, A. Gindulyte, et al., PubChem substance and compound databases, Nucleic Acids Res. 44 (2016) D1202–D1213, https://doi.org/10.1093/nar/gkv951.

[25] A. Daina, O. Michielin, V. Zoete, SwissADME: a free web tool to evaluate pharmacokinetics, drug-likeness and medicinal chemistry friendliness of small molecules, Sci. Rep. 7 (2017) 42717, https://doi.org/10.1038/srep42717.

[26] X. Li, X. Liu, F. Yang, T. Meng, X. Li, Y. Yan, et al., Mechanism of Dahuang Mudan Decotion in the treatment of colorectal cancer based on network pharmacology and experimental validation, Heliyon 10 (2024) e32136, https://doi.org/10.1016/j.heliyon.2024.e32136.

[27] S.X. Ge, D. Jung, R. Yao, ShinyGO: a graphical gene-set enrichment tool for animals and plants, Bioinformatics 36 (2020) 2628–2629, https://doi.org/10.1093/bioinformatics/btz931.

[28] I.J.L. Lagu, D.W. Nyamai, S.N. Njeru, Phytochemical analysis, in-vitro and in-silico study of antiproliferative activity of ethyl acetate fraction of *Launaea cornuta* (Hochst. ex Oliv. & Hiern) C. Jeffrey against human cervical cancer cell line, Front. Pharmacol. 15 (2024), https://doi.org/10.3389/fphar.2024.1399885.

[29] J. Jiao, C. Cheng, P. Xu, P. Yang, K. Zhang, Y. Jing, et al., Mechanisms of pancreatic tumor suppression mediated by Xiang-lian pill: an integrated in silico exploration and experimental validation, J. Ethnopharmacol. 298 (2022) 115586, https://doi.org/10.1016/j.jep.2022.115586.

[30] S.N. Njeru, J.M. Muema, In vitro cytotoxicity of *Aspilia pluriseta* Schweinf. extract fractions, BMC Res. Notes 14 (2021) 57, https://doi.org/10.1186/s13104-021-05472-4.

[31] H. Sung, J. Ferlay, R.L. Siegel, M. Laversanne, I. Soerjomataram, A. Jemal, et al., Global cancer statistics 2020: GLOBOCAN estimates of incidence and mortality worldwide for 36 cancers in 185 countries, CA A Cancer J. Clin. 71 (2021) 209–249, https://doi.org/10.3322/caac.21660.

[32] P.S. Hyeok, M. Kim, S. Lee, W. Jung, B. Kim, Therapeutic potential of natural products in the treatment of cervical cancer: a review, Nutrients 13 (2021) 154, https://doi.org/10.3390/nu14112274.

[33] M. Fridlender, Y. Kapulnik, H. Koltai, Plant derived substances with anti-cancer activity: from folklore to practice, Front. Plant Sci. 6 (2015), https://doi.org/10.3389/fpls.2015.00799.

[34] P.R. Matowa, M. Gundidza, L. Gwanzura, C.F.B. Nhachi, A survey of ethnomedicinal plants used to treat cancer by traditional medicine practitioners in Zimbabwe, BMC Complement Med Ther 20 (2020) 278, https://doi.org/10.1186/s12906-020-03046-8.

[35] Z.-S. Zhang, D. Li, L.-J. Wang, N. Ozkan, X.D. Chen, Z.-H. Mao, et al., Optimization of ethanol–water extraction of lignans from flaxseed, Separ. Purif. Technol. 57 (2007) 17–24, https://doi.org/10.1016/j.seppur.2007.03.006.

[36] A. Delazar, L. Nahar, S. Hamedeyazdan, S.D. Sarker, Microwave-assisted extraction in natural products isolation, Methods Mol. Biol. 864 (2012) 89–115, https://doi.org/10.1007/978-1-61779-624-1_5.

[37] H.M. Rashid, A.I. Mahmod, F.U. Afifi, W.H. Talib, Antioxidant and Antiproliferation activities of *Lemon Verbena* (Aloysia citrodora): an in vitro and in vivo study, Plants 11 (2022) 785, https://doi.org/10.3390/plants11060785.

[38] V. Kuete, L.P. Sandjo, B. Wiench, T. Efferth, Cytotoxicity and modes of action of four Cameroonian dietary spices ethno-medically used to treat Cancers: *Echinops giganteus, Xylopia aethiopica, Imperata cylindrica* and *Piper capense*, J. Ethnopharmacol. 149 (2013) 245–253, https://doi.org/10.1016/j.jep.2013.06.029.

[39] G. Chen, X. Li, F. Saleri, M. Guo, Analysis of flavonoids in *Rhamnus davurica* and its antiproliferative activities, Molecules 21 (2016) 1275, https://doi.org/10.3390/molecules21101275.

[40] P.S. Steeg, Tumor metastasis: mechanistic insights and clinical challenges, Nat. Med. 12 (2006) 895–904, https://doi.org/10.1038/nm1469.

[41] C.L. Chaffer, R.A. Weinberg, A perspective on cancer cell metastasis, Science 331 (2011) 1559–1564, https://doi.org/10.1126/science.1203543.

[42] M. Al-Zharani, F.A. Nasr, N. Abutaha, A.S. Alqahtani, O.M. Noman, M. Mubarak, et al., Apoptotic induction and anti-migratory effects of *Rhazya Stricta* Fruit extracts on a human breast cancer cell line, Molecules 24 (2019) 3968, https://doi.org/10.3390/molecules24213968.

[43] S. Deng, P. Yuan, J. Sun, The role of NF-κB in carcinogenesis of cervical cancer: opportunities and challenges, Mol. Biol. Rep. 51 (2024) 538, https://doi.org/10.1007/s11033-024-09447-z.

[44] J. Liu, Q. Zhang, R.-L. Li, S.-J. Wei, Y.-X. Gao, L. Ai, et al., Anti-proliferation and anti-migration effects of an aqueous extract of *Cinnamomi ramulus* on MH7A rheumatoid arthritis-derived fibroblast-like synoviocytes through induction of apoptosis, cell arrest and suppression of matrix metalloproteinase, Pharmaceut. Biol. 58 (2020) 863–877, https://doi.org/10.1080/13880209.2020.1810287.

[45] M.A. Dickson, G.K. Schwartz, Development of cell-cycle inhibitors for cancer therapy, Curr. Oncol. 16 (2009) 36–43.

[46] S. Khazaei, N.M. Esa, V. Ramachandran, R.A. Hamid, A.K. Pandurangan, A. Etemad, et al., In vitro antiproliferative and apoptosis inducing effect of *Allium atroviolaceum* Bulb extract on breast, cervical, and liver cancer cells, Front. Pharmacol. 8 (2017), https://doi.org/10.3389/fphar.2017.00005.

[47] T. Ozaki, A. Nakagawara, Role of p53 in cell death and human cancers, Cancers 3 (2011) 994–1013, https://doi.org/10.3390/cancers3010994.

[48] M. Hollstein, D. Sidransky, B. Vogelstein, C.C. Harris, p53 mutations in human cancers, Science 253 (1991) 49–53, https://doi.org/10.1126/science.1905840.

[49] G. Rescourio, A.Z. Gonzalez, S. Jabri, B. Belmontes, G. Moody, D. Whittington, et al., Discovery and in vivo evaluation of macrocyclic Mcl-1 inhibitors Featuring an α-Hydroxy Phenylacetic acid Pharmacophore or Bioisostere, J. Med. Chem. 62 (2019) 10258–10271, https://doi.org/10.1021/acs.jmedchem.9b01310.

[50] M.A. Moga, O.G. Dimienescu, C.A. Arvatescu, A. Mironescu, L. Dracea, L. Ples, The role of natural polyphenols in the prevention and treatment of cervical cancer—an overview, Molecules 21 (2016) 1055, https://doi.org/10.3390/molecules21081055.

[51] Y. Li, S.-J. Wang, W. Xia, K. Rahman, Y. Zhang, H. Peng, et al., Effects of Tatariside G isolated from *Fagopyrum tataricum* roots on apoptosis in human cervical cancer HeLa cells, Molecules 19 (2014) 11145–11159, https://doi.org/10.3390/molecules190811145.

[52] Kleszcz R, Majchrzak-Celińska A, Baer-Dubowska W. Tannins in cancer prevention and therapy. Br. J. Pharmacol. n.d.;n/a. https://doi.org/10.1111/bph.16224.

[53] P.A. Fernandes, DA e Silva, M.A. Lima, Cytotoxic effects of alkaloids on cervical carcinoma cell lines: a review, Revista de Ciências Farmacêuticas Básica e Aplicada 36 (2015).

[54] M.R. Patlolla J, V. Rao C, Triterpenoids for cancer prevention and treatment: current Status and future prospects, Chem. Pharm. Bull. 13 (2012) 147–155, https://doi.org/10.2174/138920112798868719.

[55] F.L. Hakkim, M. Al-Buloshi, J. Achankunju, Chemical composition and anti-proliferative effect of Oman's *Ganoderma applanatum* on breast cancer and cervical cancer cells, Journal of Taibah University Medical Sciences 11 (2016) 145–151, https://doi.org/10.1016/j.jtumed.2016.01.007.

[56] N. An, F. Liu, Camelliol C inhibits viability, migration, and invasion of human cervical cancer cells via induction of apoptosis, G2/M cell cycle arrest, and blocking of PI3K/AKT signalling pathway, Arch. Med. Sci. (2020), https://doi.org/10.5114/aoms.2020.95964.

[57] A.D. Herrera-España, J. Us-Martín, S. Hernández-Ortega, G. Mirón-López, L. Quijano, J.R. Villanueva-Toledo, et al., Synthesis, structure analysis and activity against breast and cervix cancer cells of a triterpenoid thiazole derived from ochraceolide A, J. Mol. Struct. 1204 (2020) 127555, https://doi.org/10.1016/j.molstruc.2019.127555.

[58] Ganesan K, Manivel A. Evaluation of anticancer activity of squalene isolated from *Canthium coromandelicum* leaves. World J. Pharmaceut. Res. n.d.;7.

[59] K.R.A. Abdellatif, R.B. Bakr, Pyrimidine and fused pyrimidine derivatives as promising protein kinase inhibitors for cancer treatment, Med. Chem. Res. 30 (2021) 31–49, https://doi.org/10.1007/s00044-020-02656-8.

[60] G.-H. Liu, T. Chen, X. Zhang, X.-L. Ma, H.-S. Shi, Small molecule inhibitors targeting the cancers, MedComm 3 (2022) e181, https://doi.org/10.1002/mco2.181.

[61] W.-I. Wu, W.C. Voegtli, H.L. Sturgis, F.P. Dizon, G.P.A. Vigers, B.J. Brandhuber, Crystal structure of human AKT1 with an allosteric inhibitor reveals a new mode of kinase inhibition, PLoS One 5 (2010) e12913, https://doi.org/10.1371/journal.pone.0012913.

[62] C.C. Kumar, V. Madison, AKT crystal structure and AKT-specific inhibitors, Oncogene 24 (2005) 7493–7501, https://doi.org/10.1038/sj.onc.1209087.

[63] B. Wilding, D. Scharn, D. Böse, A. Baum, V. Santoro, P. Chetta, et al., Discovery of potent and selective HER2 inhibitors with efficacy against HER2 exon 20 insertion-driven tumors, which preserve wild-type EGFR signaling, Nat Cancer 3 (2022) 821–836, https://doi.org/10.1038/s43018-022-00412-y.

[64] Q. Liu, S. Yu, W. Zhao, S. Qin, Q. Chu, K. Wu, EGFR-TKIs resistance via EGFR-independent signaling pathways, Mol. Cancer 17 (2018) 1–9, https://doi.org/10.1186/s12943-018-0793-1.

[65] R.R. Padala, R. Karnawat, S.B. Viswanathan, A.V. Thakkar, A.B. Das, Cancerous perturbations within the ERK, PI3K/Akt, and Wnt/β-catenin signaling network constitutively activate inter-pathway positive feedback loops, Mol. Biosyst. 13 (2017) 830–840, https://doi.org/10.1039/C6MB00786D.